

Electrochemical reduction of hydrogen peroxide on stainless steel[†]

S PATRA and N MUNICHANDRAIAH*

Department of Inorganic and Physical Chemistry, Indian Institute of Science, Bangalore 560 012
e-mail: muni@ipc.iisc.ernet.in

Abstract. Electrochemical reduction of hydrogen peroxide is studied on a sand-blasted stainless steel (SSS) electrode in an aqueous solution of NaClO₄. The cyclic voltammetric reduction of H₂O₂ at low concentrations is characterized by a cathodic peak at –0.40 V versus standard calomel electrode (SCE). Cyclic voltammetry is studied by varying the concentration of H₂O₂ in the range from 0.2 mM to 20 mM and the sweep rate in the range from 2 to 100 mV s⁻¹. Voltammograms at concentrations of H₂O₂ higher than 2 mM or at high sweep rates consist of an additional current peak, which may be due to the reduction of adsorbed species formed during the reduction of H₂O₂. Amperometric determination of H₂O₂ at –0.50 V vs SCE provides the detection limit of 5 μM H₂O₂. A plot of current density versus concentration has two segments suggesting a change in the mechanism of H₂O₂ reduction at concentrations of H₂O₂ ≥ 2 mM. From the rotating disc electrode study, diffusion co-efficient of H₂O₂ and rate constant for reduction of H₂O₂ are evaluated.

Keywords. Electrochemical reduction of H₂O₂; stainless steel electrode; cyclic voltammetry; amperometry; rotating disc electrode.

1. Introduction

Hydrogen peroxide is an important ingredient in a wide range of industrial processes such as food processing (e.g. in the cold pasteurization of milk, wine aging, etc.), textile bleaching, cosmetics preparation, pharmaceutical manufacturing, etc.¹ H₂O₂ is also an intermediates during the reduction of oxygen in fuel cells.² In fact, a challenging problem in fuel cell is the premature failure of the cell due to attack of the electrodes by H₂O₂.³ The presence of stable dioxygen intermediates is an indication of intrinsic cell inefficiency in the reduction of oxygen at the cathode. In biological aerobic organisms, energy is derived from oxygen, which is susceptible to form O₂[•], OH[•] and H₂O₂, during its reduction by the electron transfer effect of mitochondria.⁴ These radicals (reactive oxygen species) cause different kinds of disorder in the body such as Alzheimer's, myocardial infarction, atherosclerosis, Parkinson's, etc.⁵ Hence, studies on H₂O₂ reduction are important in both chemistry and biology.

Electrochemical reduction of H₂O₂ at bare electrodes has been studied by different groups.^{6–12} On Pt electrodes, pH and over-potential play important

roles on kinetics of H₂O₂ reduction.⁶ Ag electrodes exhibit autocatalytic mechanism towards the reduction of H₂O₂ in acidic electrolyte.⁷ Somasundrum *et al*⁸ studied H₂O₂ reduction on Cu metal in 0.1 M phosphate buffer solution (pH = 6.7). They reported the mechanism of H₂O₂ reduction at ambient temperature and also the effect of dissolved oxygen on H₂O₂ reduction. H₂O₂ reduction was also studied on polycrystalline copper in borax buffer in the light of surface oxidation in presence of chloride ions in the electrolyte.⁹

There are also a few reports on reduction of H₂O₂ on modified electrodes.^{10–12} PdO₂ and IrO₂ modified glassy carbon electrodes (GCE) were used as the electrodes for reduction of H₂O₂ in basic solution.¹⁰ The electrocatalytic activity of a graphite electrode modified by micro quantities of platinum metals (Pd or Pt + Pd) towards the H₂O₂ reduction were characterized by Dodevska *et al* and the electrode was used as a glucose biosensor.¹¹ A conducting polymer modified by Rh micro-particles on GCE was also used to detect H₂O₂, which was produced from the oxidation of glucose.¹²

Generally, noble metallic electrodes are used for studying electrochemical reactions because of their stability in the electrolytes. Non-noble metals are not preferred because they corrode in aqueous solutions. In the case of H₂O₂ reduction, copper was em-

[†]Dedicated to the memory of the late Professor S K Rangarajan

*For correspondence

ployed and mechanistic studies were reported.^{8,9} There are no reports on electrochemical reduction of H_2O_2 on stainless steel (SS), to the best of authors' knowledge. In the present work, SS, which is a very common alloy, is used as the electrode material for electrochemical reduction of H_2O_2 in neutral NaClO_4 electrolyte. Cyclic voltammetry, amperometry and rotating disc electrode (RDE) studies suggest that SS can be used for electrochemical determination of H_2O_2 at a concentration level as low as $5 \mu\text{M}$.

2. Experimental sections

Analytical grade H_2SO_4 , NaClO_4 , NaOH and HCl were purchased from Merck, Purified H_2O_2 (30%) was purchased also from Merck. A high purity commercial 304 grade stainless steel (SS) foil (thickness: 0.2 mm) was used as the substrate for H_2O_2 reduction. A solution of 0.5 M NaClO_4 (pH = 5.8) was usually used as the supporting electrolyte for H_2O_2 . Some experiments were also conducted by varying pH of the electrolyte. All solutions were prepared in doubly distilled water. The electrolyte solutions were de-aerated by bubbling N_2 for at least 30 min prior to electrochemical measurements. A glass cell of about 70 ml capacities with suitable ground-glass joints to introduce a working electrode, Pt foil auxiliary electrodes, and a SCE was used for electrochemical experiments. All potential values are reported against SCE.

A SS sheet was subjected to sand-blasting to generate a noticeable rough surface and washed copiously using a detergent followed by a mild etching in dilute H_2SO_4 . A foil of 7 mm width and 6 cm in length was sectioned out of a sand-blasted SS sheet, 1.4 cm^2 areas at one of the ends was exposed to the electrolyte and the rest of its length was used as a tag for taking electrical contacts. Hereafter, sand-blasted SS electrode is hereafter referred to as SSS. The SSS substrate was again washed thoroughly, rinsed with acetone and dried in vacuum at ambient temperature for about 30 min for further studies. Geometric area of the electrode was used for calculation of current density (mA cm^{-2}).

Cyclic voltammetry and amperometry experiments were carried out using an EG&G PARC potentiostat/galvanostat Versastat II or Eco Chemie potentiostat/galvanostat model Autolab 30. RDE experiments were carried out using Eco Chemie RDE model Rotator 188. The electrode tip was

made of SS. Experiments were carried out with rotation speed in the range from 100 to 5000 rpm.

3. Results and discussions

3.1 Cyclic voltammetry

Cyclic voltammogram of a SSS electrode recorded in 0.5 M NaClO_4 + 5 mM H_2O_2 at 5 mV s^{-1} in the potential range from -0.1 to -0.7 V is shown in figure 1. For comparison purpose, cyclic voltammogram recorded in 0.5 M NaClO_4 in the absence of H_2O_2 is also presented. In the absence of H_2O_2 , cyclic voltammogram (figure 1 curve (i)) does not exhibit any current peak suggesting that SSS is stable in the potential range studied. In the presence of H_2O_2 in the electrolyte, however, current starts increasing at -0.1 V (figure 1 curve (ii)) in the forward sweep. On further extending the sweep in the negative direction, a reduction current peak (P1) appears at -0.404 V. On reversing the direction of sweep at -0.7 V, no oxidation current peak is observed. The appearance of an irreversible reduction peak in the presence of H_2O_2 (figure 1 curve (ii)) and absence of peak in the absence of H_2O_2 (figure 1 curve (i)) suggest that the current peak P1 is due to reduction of H_2O_2 . In order to examine the effect of roughness of SSS surface due to sand blasting on the reduction of H_2O_2 , a cyclic voltammogram recorded using a plain SS is shown in figure 1

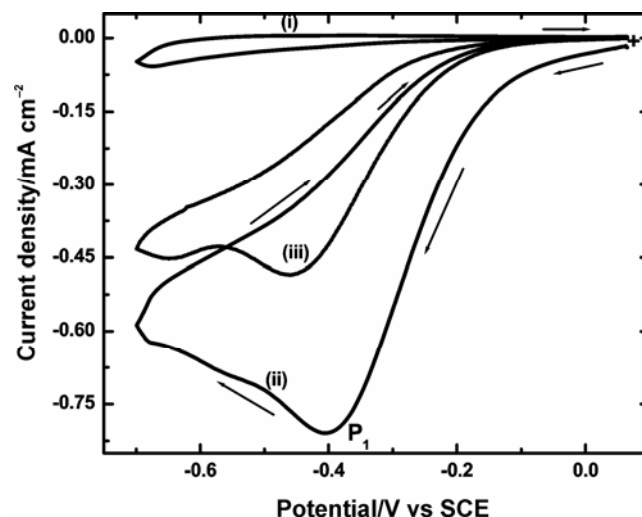


Figure 1. Cyclic voltammograms of SSS electrode in 0.5 M NaClO_4 in the absence of H_2O_2 (i) and presence of 5 mM H_2O_2 (ii); and voltammogram of SS electrode in 0.5 M NaClO_4 + 5 mM H_2O_2 (iii). Sweep rate: 5 mV s^{-1} .

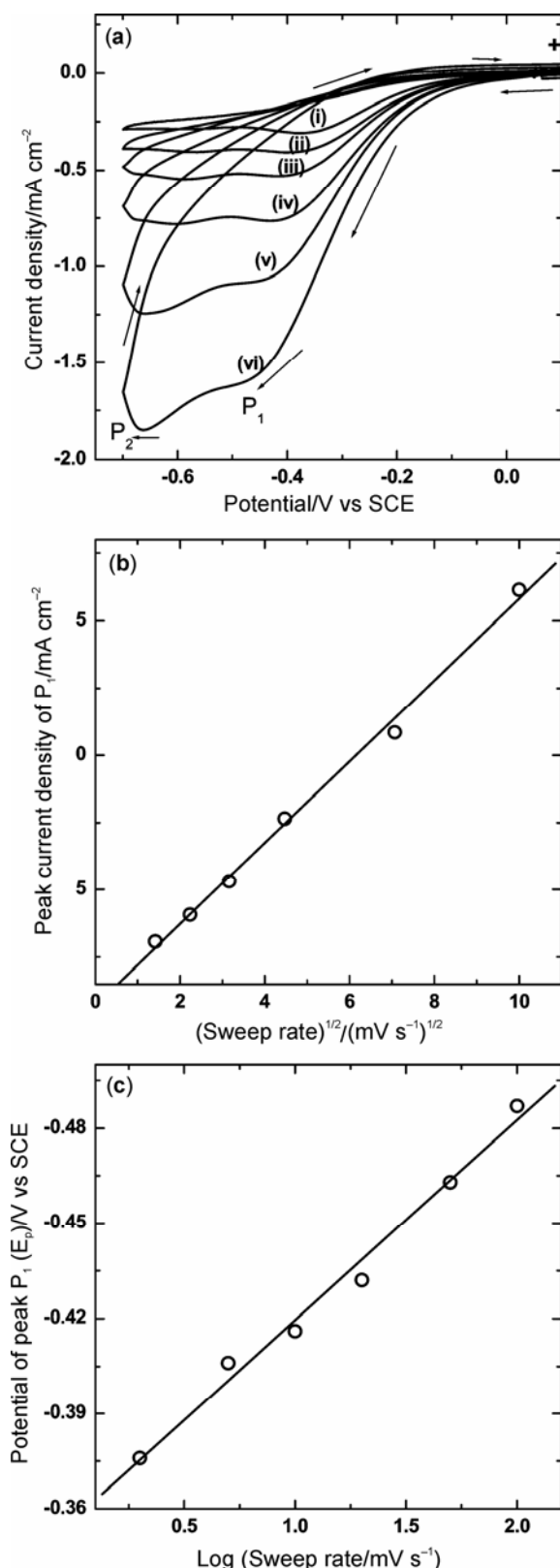


Figure 2. (a) Cyclic voltammograms of SSS electrode in 0.5 M NaClO₄ + 3 mM H₂O₂ at a sweep rate of 2 (i), 5 (ii), 10 (iii), 20 (iv), 50 (v) and 100 mV s⁻¹ (vi); (b) The peak current density of P₁ versus (sweep rate)^{1/2} of data presented in (a); and (c) potential of peak P₁ versus log (sweep rate).

(curve (iii)). It is observed that the voltammograms on SSS and SS are similar in shape and the peak current density on SSS is 60% greater than on SS (figure 1). This indicates a 60% increase in surface area of SSS due to sand-blasting. These results further suggest that basically the SS surface facilitates the electrochemical reduction of H₂O₂. For further studies, SSS was used. A SSS electrode was repeatedly cycled in 0.5 M NaClO₄ + 4 mM H₂O₂ at 5 mV s⁻¹, to examine its stability and activity towards reduction of H₂O₂. Cyclic voltammograms (not shown), similar to figure 1 curve (ii), were reproducible with very marginal decrease in peak current during ten cycles. Although the supporting electrolyte, namely, 0.5 M NaClO₄ is not a buffer solution and the surface concentration of OH⁻ ions increases during H₂O₂ reduction by cyclic voltammetry, the voltammograms are not affected to a considerable extent. Buffer solutions are not used as the supporting electrolytes to avoid any adsorption effects on the SSS surface. Thus SSS is considered to retain its electrochemical activity for reduction of H₂O₂ without undergoing fouling or poisoning due to any intermediate species adsorbed during the reduction process in the supporting electrolyte.

Cyclic voltammograms of SSS electrode in 0.5 M NaClO₄ + 3 mM H₂O₂ were recorded at different sweep rates (ν) and the data are shown in figure 2(a). At low sweep rates (figure 2(a) curve (i)), there is single reduction current peak (P₁) appearing at about -0.376 V. As the sweep rate increases, however, another reduction peak (P₂) starts appearing and it becomes a clear, sharp peak at high sweep rates. At 100 mV s⁻¹, for instance, the peak P₂ is clearly seen at -0.66 V. The appearance of P₂ is likely to be due to reduction of intermediate species adsorbed on the SSS surface during H₂O₂ reduction, as discussed below. The variation of peak current density (I_{p1}) of P₁ with $\nu^{1/2}$ is shown in figure 2(b). There is a linear increase of I_{p1} with $\nu^{1/2}$, suggesting that the reduction of H₂O₂ on SSS is diffusion controlled. The relationship between E_p and sweep rate (ν) for an irreversible reaction is given by (1).¹³

$$E_p = k + (2.3RT/(2n_a\alpha_aF))\log \nu, \quad (1)$$

where k is a constant, α_a is transfer co-efficient, n_a is number of electrons transferred up to the rate determining step of the reaction and the other symbols have their usual meanings. The product $(2.3RT/(n_a\alpha_aF))$ is equivalent to the Tafel slope, which can

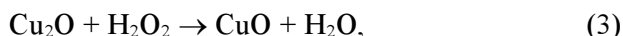
be evaluated from (1). A plot of E_p vs $\log v$ is shown in figure 2(c). The value of slope of this plot obtained is 0.12 V. Thus, the Tafel slope is 0.24 V. This value is greater than 0.12 V, which is generally expected for a single electron transfer process (assuming transfer coefficient (α) equal to 0.5). As the electrochemical reduction of H_2O_2 on SSS appears to have a complicated mechanism as discussed later, α is calculated from cyclic voltammograms using (2).

$$E_p - E_{p/2} = 1.857RT/(\alpha nF), \quad (2)$$

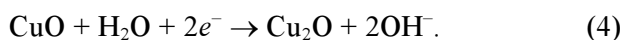
where $E_{p/2}$ is the potential on rising part of the voltammogram corresponding to one half the peak current, n is the number of electron in rate determining step and the rest of the symbols have their usual meanings. The value of α obtained is 0.32. As the value of Tafel slope is high and the value of α is low, the mechanism of H_2O_2 reduction appears to be complex.

Cyclic voltammograms of an SSS electrode were recorded in 0.5 M $NaClO_4$ solution containing H_2O_2 at various concentrations. Some of the voltammograms are presented in figure 3(a). There is an increase in current with increasing concentration of H_2O_2 . At low concentrations of H_2O_2 , single reduction peak P_1 appears at about -0.5 V (figure 3(a) curve (ii)). However, the second peak P_2 is observed at high concentration of H_2O_2 (figure 3(a) curve (iv)). A plot of I_{p1} versus concentration is shown in figure 3(b). There is a linear increase of I_{p1} with an increase in concentration of H_2O_2 . These results suggested that SSS is an appropriate electrode material for studying electrochemical reduction of H_2O_2 .

Studies on mechanism of electrochemical reduction of H_2O_2 on different metallic electrodes occupied interest in the literature. Mechanistic studies were conducted on polycrystalline copper in a borax buffer electrolyte.⁹ Copper electrode was shown to consist of CuO and Cu_2O layers. The oxides of Cu are considered to catalyse the reduction of H_2O_2 . The proposed mechanism involves the chemical oxidation of Cu_2O by H_2O_2 :



which is followed by electrochemical reduction of CuO to Cu_2O as



Thus, the H_2O_2 reduction occurs indirectly with Cu_2O acting as a redox carrier. Cyclic voltammetric peak currents correspond to the reduction of CuO .⁹ Furthermore, it was considered that CuO surface inhibits direct electron transfer to H_2O_2 for reducing the latter. Rate of the reaction was considered to be determined by the surface coverage of CuO .

Similar to the above mechanism of reduction of H_2O_2 mediated by CuO , a mechanism mediated by IrO_2 on glassy carbon electrode was also proposed.¹⁰ An auto catalytic mechanism on Ag electrode was

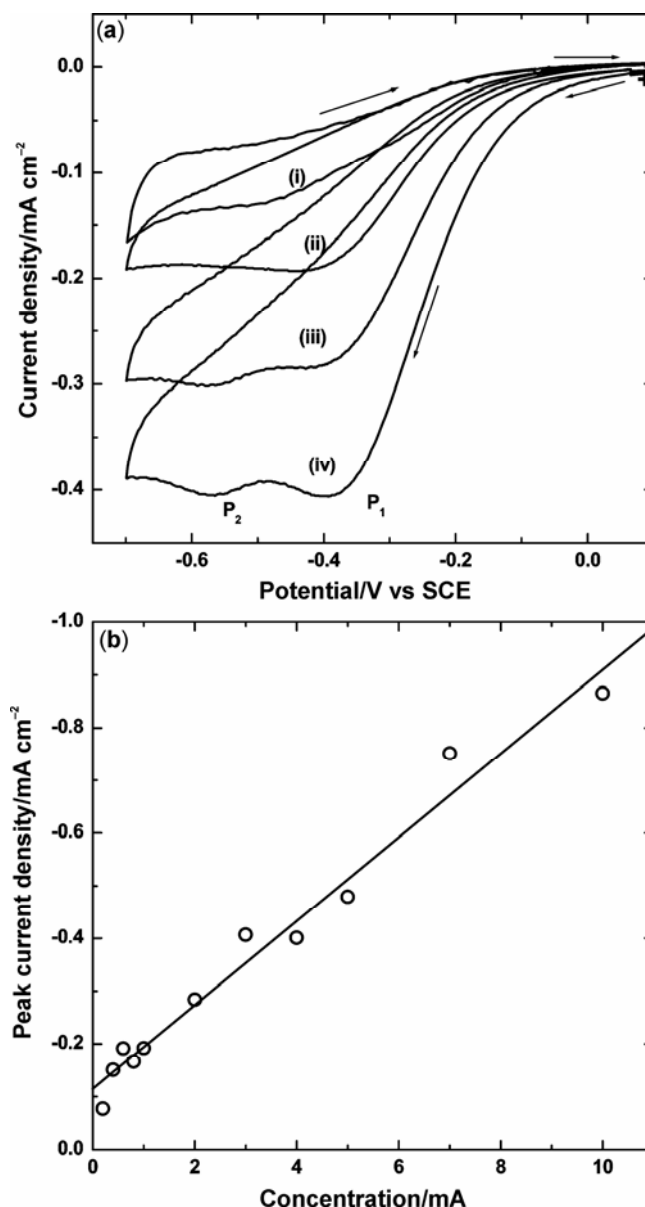
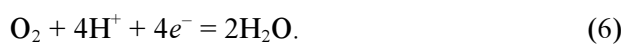


Figure 3. (a) Cyclic voltammograms of SSS electrode at a sweep rate of 5 mV s^{-1} in 0.5 M $NaClO_4$ with 0.8 (i), 1 (ii), 2 (iii), 3 (iv), 4 mM (v) of H_2O_2 ; and (b) peak current density of P_1 vs concentration of H_2O_2 .

proposed.⁷ The autocatalytic mechanism involving adsorbed OH_{ads} species was shown operative at potentials of about -0.3 V vs MSE (Hg/HgSO_4 , K_2SO_4 (sat)) reference electrode, whereas the normal mechanism is operative at -0.4 V versus MSE.

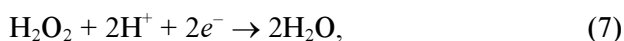
In the present study of H_2O_2 reduction on SSS, the mechanism of the reaction is different from the above discussion. Although the SSS substrate is subjected to acidic etching to remove surface oxide layers, it is likely that the surface is covered with an oxide layer (perhaps chromium oxide) before it is used for electrochemical experiments. Nevertheless, the cyclic voltammograms of SSS in H_2O_2 -free NaClO_4 electrolyte (figure 1 curve (i)) indicate the absence of any reduction current peaks. Thus, reduction of H_2O_2 on SSS is not mediated by surface oxide layers, unlike mediation of the reduction by CuO present on Cu .

A mechanism involving decomposition (or disproportionation) of H_2O_2 leading to the formation of O_2 followed by the electrochemical reduction of O_2 is also reported in the literature.^{14,15}

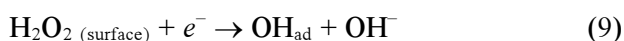
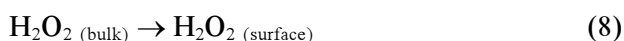


In order to examine the possibility of the above reaction, cyclic voltammograms of the SSS electrode were recorded in NaClO_4 saturated with O_2 gas. A peak corresponding to the reduction of O_2 appeared at about -0.2 V, which is more positive to -0.40 V observed for H_2O_2 reduction (figure 1 curve (ii)). Therefore disproportionation pathway for H_2O_2 reduction is ruled out. The possible mechanism, therefore, is as follows:

The direct reduction of H_2O_2 in a slightly acidic medium ($\text{pH} = 5.8$):



can be considered to occur through the formation of adsorbed OH_{ad} species.



Diffusion of H_2O_2 from bulk to the electrode surface (step 8) followed by electrontransfer steps (reactions 9 and 11) is expected to result in the cyclic voltammetric peak current. OH^- ion thus formed combine with H^+ ion (reaction 10) at the electrode to produce the reaction product, namely, H_2O . Alternately, OH_{ad} can simultaneously accept an electron and H^+ ion producing H_2O in reaction 12. It is likely that at low sweep rates and low concentrations, where a single voltammetric peak is observed, steps 10–11 are appropriate to complete the overall reduction of H_2O_2 . At high sweep rates and high concentrations of H_2O_2 , step 12 also occurs together with step 9–11, due to high surface coverage of OH_{ad} . The step 12 is likely to be responsible for the presence of second voltammetric peak (P_2) at -0.66 V.

3.2 Amperometry

In an amperometry experiment, current flowing through an SSS electrode at -0.50 V was measured as a function of concentration of H_2O_2 in 0.5 M NaClO_4 (figure 4(a)). The electrolyte was stirred uniformly by a PTFE covered magnetic bar during the experiment. A wide concentration range from $5 \mu\text{M}$ to 20 mM was studied. Subsequent to each addition of H_2O_2 , the SSS electrode shows a rapid response in increasing the current. However, current tends to decrease with time at a given concentration of H_2O_2 in the electrolyte due to adsorption of the reaction intermediate as discussed in cyclic voltammetric studies. Current was measured 5 min after each addition of H_2O_2 (figure 4a), and the amperometric current density measured from figure 4(a) is shown in figure 4(b) as a function of concentration of H_2O_2 . There are two linear segments of the data. The first segment between $5 \mu\text{M}$ and 2.5 mM is steeper than the second segment between 2.5 mM and 20 mM. Appearance of two segments is attributed to differences in surface coverage of OH_{ad} (reaction 9) at low and high concentration ranges of H_2O_2 . Thus, the rate of H_2O_2 reduction in lower concentration range is higher than the rate in higher concentration range. The rate of reduction is given by

$$i = nFk\theta C^0 \quad (13)$$

where i is the current density, k the rate constant, θ the surface coverage by adsorbed species and C^0 the

concentration of H_2O_2 in the electrolyte. The values of $k\theta$ obtained at -0.50 V are 1.15×10^{-2} and $1.02 \times 10^{-3} \text{ cm s}^{-1}$, respectively, for low and high concentration regions. This study supports the cyclic voltammetric study, where two different processes depending on concentration range and sweep rate range are possible. The linear segment in figure 4(b) in lower concentration range is likely to be due to the direct addition of electron to H_2O_2 (reaction 9)

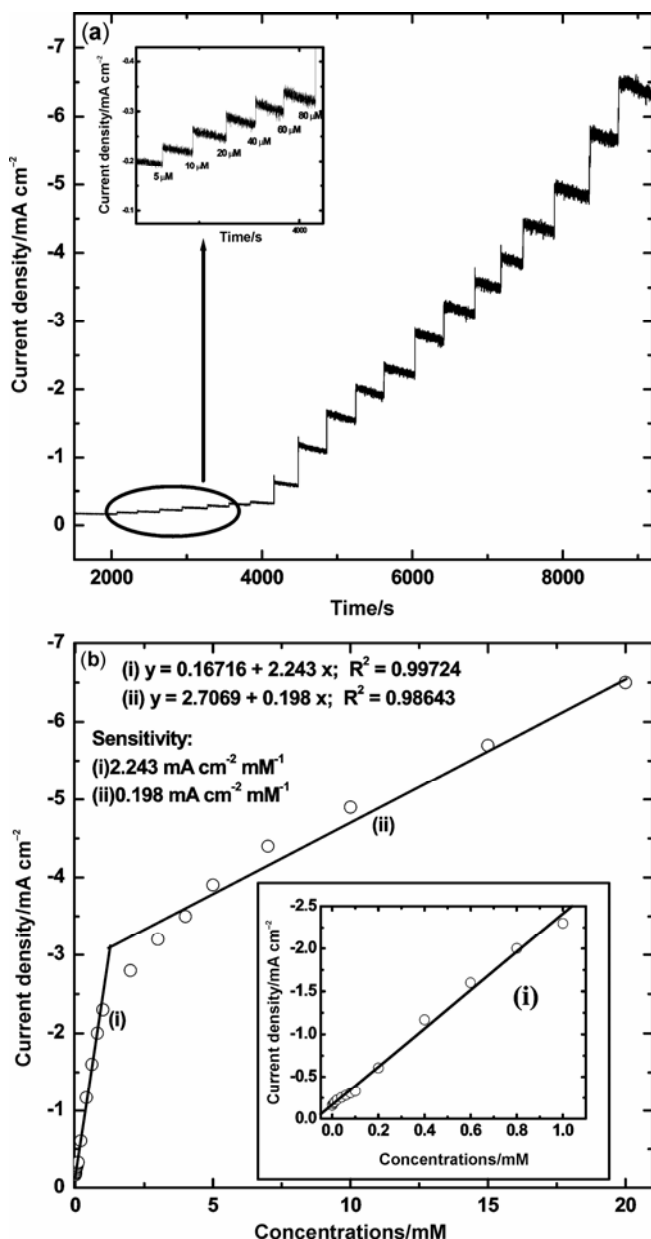


Figure 4. (a) Amperometry of SSS electrode in 0.5 M NaClO_4 with addition of different amounts of H_2O_2 . The data corresponding to low concentration range are shown as the inset in an expanded scale; and (b) current density versus concentration of H_2O_2 added (from a). The low concentration data are magnified and shown in the inset.

or to OH_{ad} (reaction 11) because of low surface coverage. However at high concentrations of H_2O_2 , the surface coverage is large and therefore the electron transfer and also the addition of H^+ to OH_{ad} can take place simultaneously (reaction 11).

3.3 Effect of electrolyte pH

The influence of pH of NaClO_4 on the reduction of H_2O_2 was examined. For this purpose 0.5 M NaClO_4 ($\text{pH} = 5.8$) was prepared and pH was adjusted to the required value by adding dilute NaOH or dilute HClO_4 . Cyclic voltammogram of an SSS in electrolytes consisting of 4 mM of H_2O_2 are shown in figure 5. At low pH value ($\text{pH} = 1.5$), no peak was observed probably due to the decomposition of H_2O_2 . At $\text{pH} = 2.5$, there are two reduction peaks (P_1 and P_2) with peak potentials at -0.17 and -0.50 V, respectively. When pH is increased to 5.8 , there is a shift in peak potentials to -0.40 and -0.66 V, respectively, for P_1 and P_2 . The variation of potential of a H^+ ion-dependent process (reaction 7) is 0.059 V per unit pH according to the Nernst equation. For the increase of pH from 2.5 to 5.8 , a shift of potential in the negative direction by 0.195 V is expected. Accordingly, there is a large shift in potentials of peaks P_1 and P_2 by changing the pH from 2.5 to 5.8 . Single cyclic voltammetric peaks are observed in electrolytes of pH values 10 and 11 (figure 5d and e). A plot of I_{p1} versus pH (figure 5f) shows that the rate of H_2O_2 reduction is maximum at $\text{pH} = 5.8$, and it decreases by either decreasing or increasing pH from 5.8 .

3.4 Rotating disc electrode studies

Experiments were carried out by subjecting a RDE made of SS to a linear sweep voltammetry at a sweep rate of 5 mV s^{-1} in 0.5 M NaClO_4 consisting of H_2O_2 at varying concentrations. The speed of RDE was varied from 100 to 3000 rpm. A typical set of data obtained in $0.5 \text{ M NaClO}_4 + 1 \text{ mM H}_2\text{O}_2$ with several rotation speeds are shown in figure 6(a). Current starts increasing at about -0.4 V and reaches a plateau in the potential range between -0.65 and -0.85 V. The plateau region commences at less negative potential if the speed is low, whereas it commences at more negative potential if the RDE speed is high. There is an increase in plateau current with increasing speed of rotation. The plateau current, which is generally known as limiting current

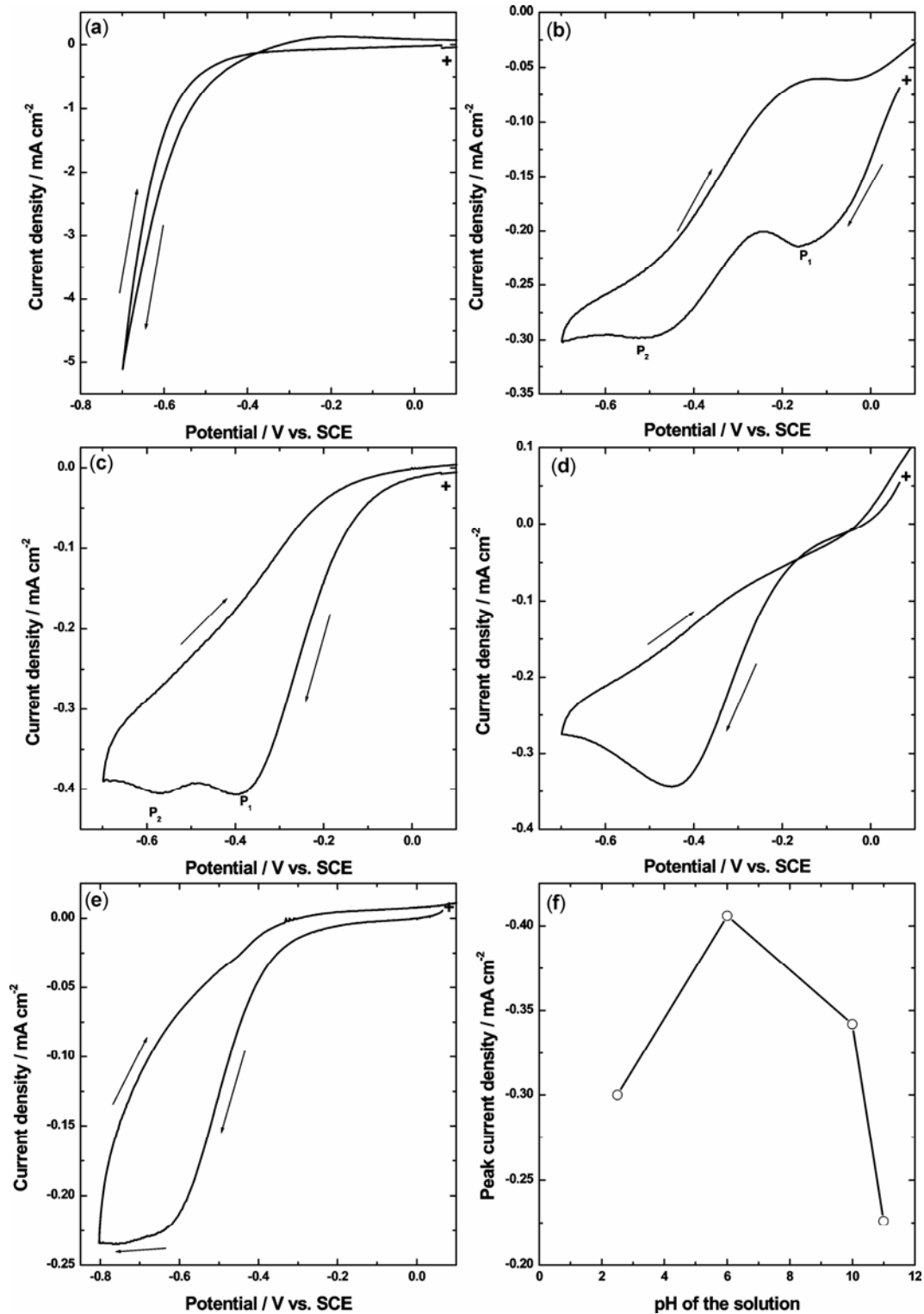


Figure 5. Cyclic voltammograms of SSS in 3 mM H₂O₂ and 0.5 M NaClO₄ of pH (a) 1.5, (b) 2.5, (c) 5.8, (d) 10.0 and (e) 11.0 and (f) current density of peak P₁ versus pH of the solution.

density (i_L) is related to rotation rate by Levich equation:¹⁷

$$i_L = 0.62nFAD^{1/2}\nu^{-1/6}C^0\omega^{1/2}, \quad (14)$$

where ν is kinematic viscosity of the medium, ω ($= 2\pi f$) is angular velocity, f is frequency in revolution per second and other symbols have their usual significance. Plots of i_L versus $f^{1/2}$ were constructed

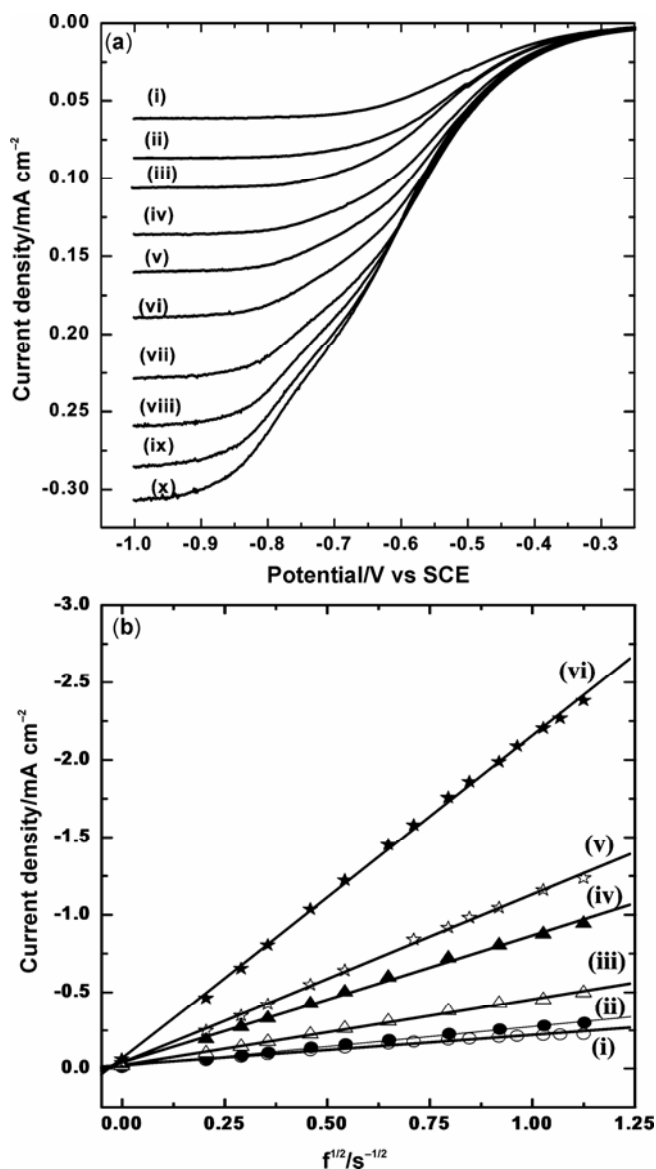


Figure 6. (a). Linear sweep voltammograms of SS rotating disk electrode in 0.5 M NaClO₄ + 1 mM of H₂O₂ with speed of rotation of 100 (i), 200 (ii), 300 (iii), 500 (iv), 700 (v), 1000 (vi), 1500 (vii), 2000 (viii), 2500 (ix), 3000 rpm (x); and (b). Levich plot for H₂O₂ concentration of 0.8 (i), 1 (ii), 2 (iii), 3 (iv), 5 (v), 10 mM (vi).

from the data measured in electrolytes of different concentrations of H₂O₂ and presented in figure 6(b). All plots are linear suggesting that the RDE data follow Levich relationship for all concentrations studied. Adsorption effects are considered to be absent due to high rotation speeds of RDE and therefore θ is not included in (14). From the slopes of the plots and (14), the values of apparent diffusion coefficient (D) of H₂O₂ are calculated and the average value is about $1.53 \times 10^{-6} \text{ cm}^2 \text{ s}^{-1}$. These studies further confirm that SS substrate is quite suitable for studying the electrochemical reduction of H₂O₂.

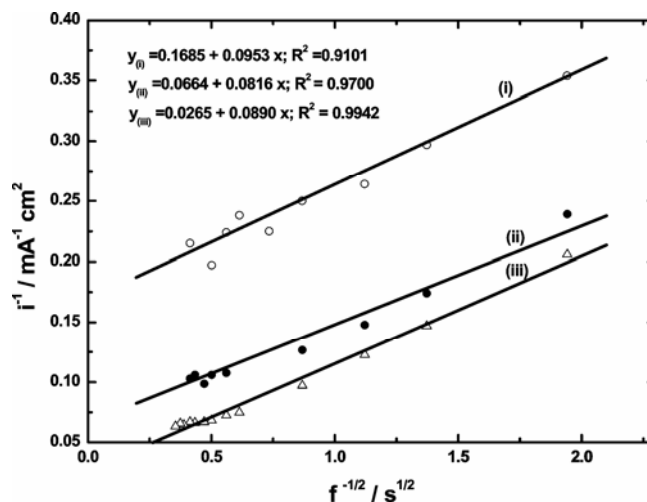


Figure 7. Koutecky–Levich plots for H₂O₂ reduction current at -0.50 (i), -0.60 (ii) and -0.70 V (iii) in 0.5 M NaClO₄ + 10 mM H₂O₂.

The RDE data were further analysed using (14) for irreversible reactions.¹⁸

$$1/i = (1/(nFkC^0)) + (1.61\nu^{1/2}/(nFC^0D^{2/3}\omega^{1/2})), \quad (15)$$

where k is rate constant. From the RDE data measured in 10 mM H₂O₂ + 0.5 M NaClO₄ electrolyte, current density measured at -0.50, -0.60 and -0.70 V (figure 6(a)) were used to plot i^{-1} versus $\omega^{-1/2}$ as shown in figure 7 (curves i, ii and iii). By extrapolation of the linear plots to origin ($\omega \rightarrow$ infinity), the values of rate constants (k) are calculated as 3.01×10^{-3} , 7.85×10^{-3} and $19.5 \times 10^{-3} \text{ cm s}^{-1}$, respectively, at -0.50 -0.60 and -0.70 V. The value of $k\theta$ calculated from amperometry at -0.50 V is comparable to this value.

4. Conclusions

Electrochemical reduction of H₂O₂ was studied on a common alloy, namely, stainless steel in 0.5 M NaClO₄ aqueous solution of pH 5.8. Cyclic voltammograms consisted of single reduction peak at low concentrations of H₂O₂ and low sweep rates, whereas they consisted of two peaks at high concentrations of H₂O₂ and high sweep rates. This was attributed to a change in mechanism of reduction. This was supported by amperometric data, wherein a plot of current versus concentration consisted of two linear segments. The detection limit obtained was 5 μM H₂O₂. The RDE studies suggested that H₂O₂ reduction was diffusion controlled.

References

1. Douglass W C 2003 *Hydrogen peroxide medical miracle* (Panama, Republic of Panama: Rhino Publishing)
2. Wilshire J and Sawyer D T 1979 *Acc. Chem. Res.* **12** 105
3. Yeager E 1980 *Progress in batteries and solar cells* (Cleveland: JEC Press) vol. 3, p 238
4. Sies H 1985 *Oxidative stress* (London: Academic Press) p. 1
5. Sies H 1986 *Angew. Chem. Int. Ed. Engl.* **25** 1058
6. Mukoyama Y, Nakanishi S, Konishi H, Karasumi K and Nakato Y 2001 *Phys. Chem. Chem. Phys.* **3** 3284
7. Flatgen G, Wasle S, Lubke M, Eickes C, Radhakrishnan G, Doblhofer K and Ertl G 1999 *Electrochim. Acta* **44** 4499
8. Somasundrum M, Kirtikara K and Tanticharoen M 1996 *Anal. Chim. Acta* **319** 59
9. Vazquez M V, de Sanchez S R and Schiffrin D J 1994 *J. Electroanal. Chem.* **374** 179
10. Cox J A and Jaworski R K 1990 *J. Electroanal. Chem.* **281** 163
11. Dodevska T, Horozova E and Dimcheva N 2006 *Anal. Bioanal. Chem.* **386** 1413
12. Arjsiriwat S, Tanticharoen M, Kirtikara K, Aoki K and Somasundrum M 2000 *Electrochem. Commun.* **2** 441.
13. Greef R, Peat R, Peter L M, Pletcher D and Robinson J 1985 *Instrumental methods in electrochemistry* (Chichester, UK: Ellis Horwood Ltd.)
14. Prabhu V G, Zarpakar L R and Dhaneswar R G 1981 *Electrochim. Acta* **26** 725
15. Somasundrum M, Tongta A, Tanticharoen M and Kirtikara K 1997 *J. Electroanal. Chem.* **440** 259
16. Honda M, Kodera T and Kita H 1986 *Electrochim. Acta* **31** 377
17. Bard A J and Faulkner L R 1990 *Electrochemical methods: Fundamental and applications* (New York, USA: John Wiley & Sons) p 218
18. Zurilla R W, Sen R K and Yeager E 1978 *J. Electrochem. Soc.* **125** 1103